

Synthesis and Characterization of Single Crystalline Hafnium Carbide Nanowires

Jinshi Yuan,^{‡,§} Han Zhang,[¶] Jie Tang,^{‡,§,†} Norio Shinya,[‡] Kiyomi Nakajima,[‡] and Lu-Chang Qin^{||,†}

[‡]National Institute for Materials Science, Tsukuba 305-0047, Japan

[§]Graduate School of Pure and Applied Sciences, University of Tsukuba, Tsukuba 305-8577, Japan

[¶]International Center for Young Scientist, National Institute for Materials Science, Tsukuba 305-0047, Japan

^{||}Department of Physics and Astronomy, Curriculum in Applied Sciences and Engineering, University of North Carolina at Chapel Hill, Chapel Hill, North Carolina 27599-3255

Hafnium carbide (HfC) is the most refractory compound known to mankind. A catalyst-assisted chemical vapor deposition method has been applied to synthesize contaminant-layer-free single crystalline HfC nanowires. The nanowires have diameter of 20–80 nm and length of several tens of microns. High-resolution transmission electron microscope images and electron diffraction patterns show that most of the nanowires grew in the <100> direction. Morphological and compositional analyses confirmed that the nanowire growth followed the vapor-liquid-solid mechanism. Field ion microscopy has also been used to reveal the surface structure of the tip of the nanowires.

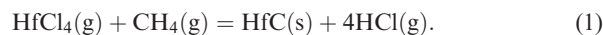
I. Introduction

HAFNIUM carbide (HfC) is the most refractory material known to date with a melting point of 3887°C, which is higher than that of both tungsten (W) and graphite at ambient conditions. This metallic compound shows very attractive properties, including low electric resistivity, low work function, high mechanical strength, high chemical stability, and high wear resistance.^{1–3} The bulk form of HfC has been widely used to bear shock and structural loads and to resist high-temperature oxidation corrosion in extreme environments, such as in the nuclear fusion reactors and rocket engines.^{4,5} The fibrous form of HfC is often used as a structural reinforcement in high-temperature composite materials.^{6,7} Considerable efforts have also been devoted to applying HfC as cold field emission cathodes. It has been demonstrated that the low work function of HfC (3.1 eV) offers an electron emission with higher brightness and lower energy spread as compared with the conventional W emitters that has a work function of 4.5 eV. Its high mechanical hardness and low surface mobility can reduce the impact of residual gas adsorption and ion bombardment, giving rise to an improved emission current stability.⁸ These HfC emitters were realized by either HfC coatings on preformed nano-protrusions or electrochemically etched tips made from a single crystal needle.^{3,9–13} On the other hand, one-dimensional nanowires have large specific surface area, high aspect ratio, and extremely low dislocation density.¹⁴ It is therefore expected that the HfC nanowire filler-reinforced composite

should greatly improve its mechanical strength as compared with its fiber filler counterparts. Moreover, the HfC nanowires can be utilized to produce electric-field-induced electron emitters or nano-electrodes. Although the synthesis of many other transition metal carbide (TMC) nanowires has been reported, no HfC nanowires have been successfully synthesized.^{15–17} We herein report a chemical vapor deposition (CVD) method to synthesize single-crystalline HfC nanowires with diameter in the range of 20–80 nm and length of a few tens of microns. We will also present structural characterization as well as the growth mechanism.

II. Experimental Procedure

In our experiment, hafnium tetrachloride (HfCl₄) and methane gases were used as reagents. The synthesis is based on the following chemical reaction similar to what we have developed to grow rare-earth boride nanowires^{18–20}:



The reaction was conducted in a quartz tube furnace with diameter of 64 mm, which was evacuated to below 10⁻¹ Pa first. HfCl₄ powders (99.95% purity; Sigma-Aldrich Japan Co.LLC, Tokyo, Japan) was put in the low-temperature zone and evaporated before temperature at the central part of the furnace was raised to 1280°C from room temperature. A schematic illustration of the synthesis system is shown in Fig. 1. The vapor was carried into the reaction zone by the flow of hydrogen (H₂) gas at a rate of 1 L/min. CH₄ gas at a flow rate of 20 mL/min was then allowed into the reaction zone through a thinner quartz tube. The gases reacted on a graphite substrate on which nickel (Ni) nanoparticles with diameter of several tens of nanometers were dispersed as catalyst. Graphite was selected to reduce possible contaminations at such a high temperature and due to the presence of corrosive HCl gas. After the reactions completed, HfC nanowire forest was grown on the substrate. The substrate and HfC nanowires were subsequently examined using scanning electron microscopy (SEM; JSM-6500F; JEOL Ltd, Tokyo, Japan) and transmission electron microscopy (TEM; JEOL-2100F; JEOL Ltd), both of which were equipped with an energy-dispersive X-ray spectrometer (EDS).

III. Results and Discussion

(1) Morphology and Structure

Figure 2(a) is an SEM image showing a dense forest of HfC nanowires grown on the substrate. The nanowires are straight and of several tens of microns in length. The EDS

R. Riedel—contributing editor

Manuscript No. 30937. Received January 11, 2012; approved April 08, 2012.

[†]Authors to whom correspondence should be addressed. e-mails: lcqin@email.unc.edu and tang.jie@nims.go.jp

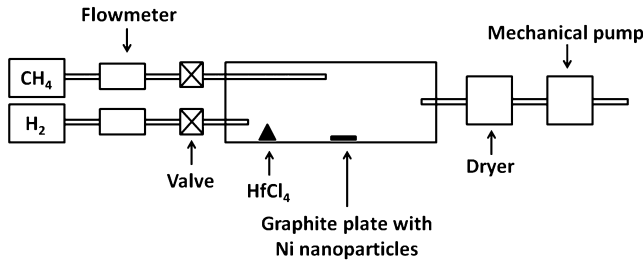


Fig. 1. Schematic of the synthesis system for producing HfC nanowires. A graphite plate was used as substrate on which Ni nanoparticles were dispersed. It was placed at the central part of the tube furnace. HfCl₄ was kept in the low temperature zone where temperature was 200°C, while the temperature of the central part reached 1280°C. H₂ was used to carry HfCl₄ vapors onto the substrate at rate of 1 L/min. CH₄ was introduced to the substrate at 20 mL/min.

spectrum given in Fig. 2(b) showed that only Hf and C elements were detected. The atomic ratio of Hf to C is nearly 1:1, indicating stoichiometric composition of the nanowire. A small part of the substrate was cut off for X-ray diffraction (XRD) examination. The XRD pattern is shown in Fig. 2(c). The XRD result showed that the sample was mainly composed of graphite and HfC. There was also some HfO₂ detected, which is attributed to the presence of O₂ inside the quartz tube leaked into the system and reacted with Hf. Figure 3(a) shows the typical morphology of a single HfC nanowire, which has a thickness of 30 nm. The inset of

Fig. 3(a) is a selected-area electron diffraction (SAED) pattern taken from the body of the nanowire, which clearly reveals its single crystallinity and growth direction. The reflections are all elongated into streaks perpendicular to the [100] lattice direction, indicating that the nanowire grows in the [100] direction. Figure 3(b) is a high-resolution TEM (HRTEM) image showing the surface profile of the same HfC nanowire. The atomically resolved lattice image also confirmed the [100] growth direction of the nanowire. In addition, the TEM image shows that the surface of the as-synthesized HfC nanowire is atomically clean. This is strikingly different from other transition metal carbide nanowires synthesized through other methods.^{15–17} A small number of nanowires grown in the [110] directions were also observed. Figures 3(c) and (d) show their typical morphology and HRTEM image, respectively.

(2) Growth Mechanism

In our synthesis, the nanowires are proposed to grow based on vapor-liquid-solid (VLS) mechanism, which was initially established by Wagner and is believed to be responsible for most of whisker growth.²¹ In the VLS growth mechanism, the growth process is described in three major steps: (1) formation of catalyst droplets, (2) the catalyst droplets adsorb reaction product and reach supersaturation, and (3) growth of whiskers with continuous condensation of product on the interface. A hemispherical tip with a catalyst particle is usually taken as the evidence of this mechanism. However, few of the HfC nanowires obtained in our experiment ended up

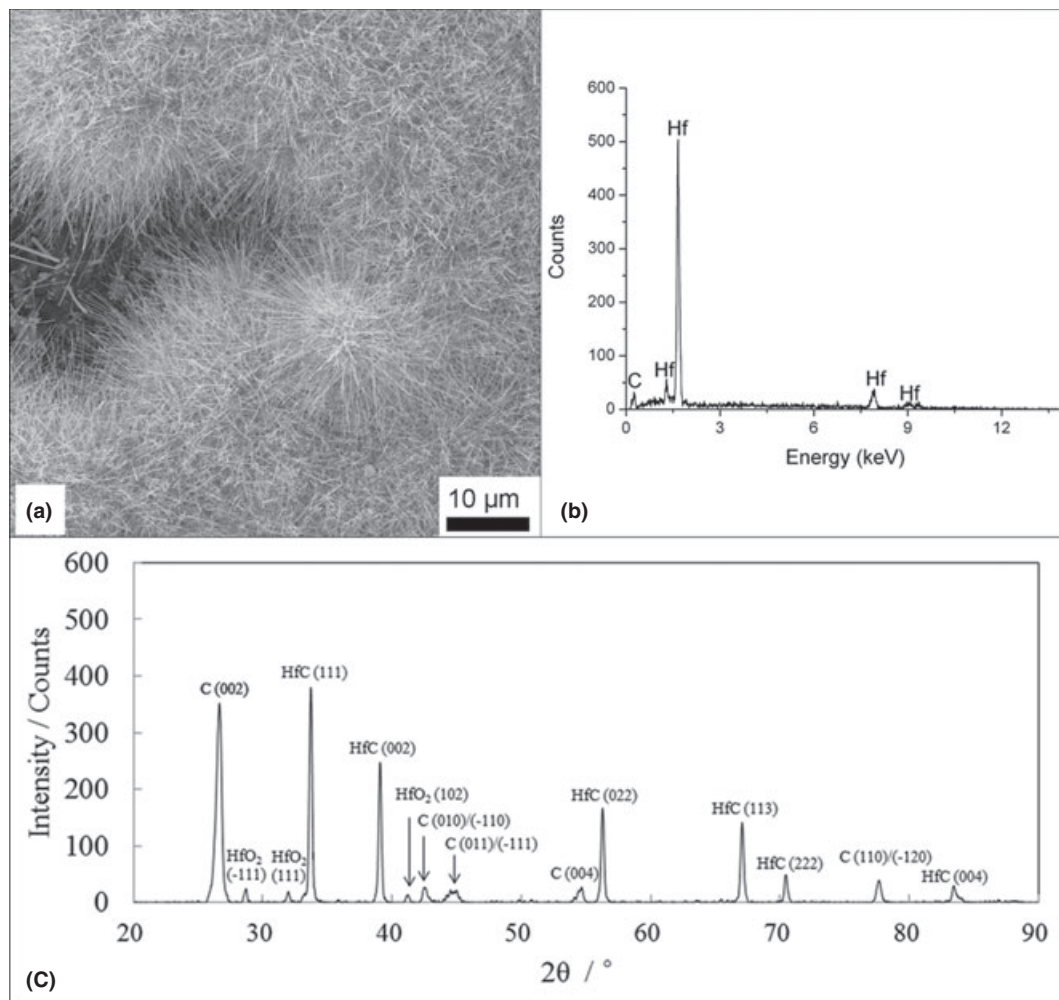


Fig. 2. (a) SEM image of the HfC nanowires grown on graphite substrate. (b) EDS analysis of the nanowires grown on the substrate showing composition of Hf and C only. (c) XRD pattern collected from a part of the substrate, which showed mainly graphite and HfC.

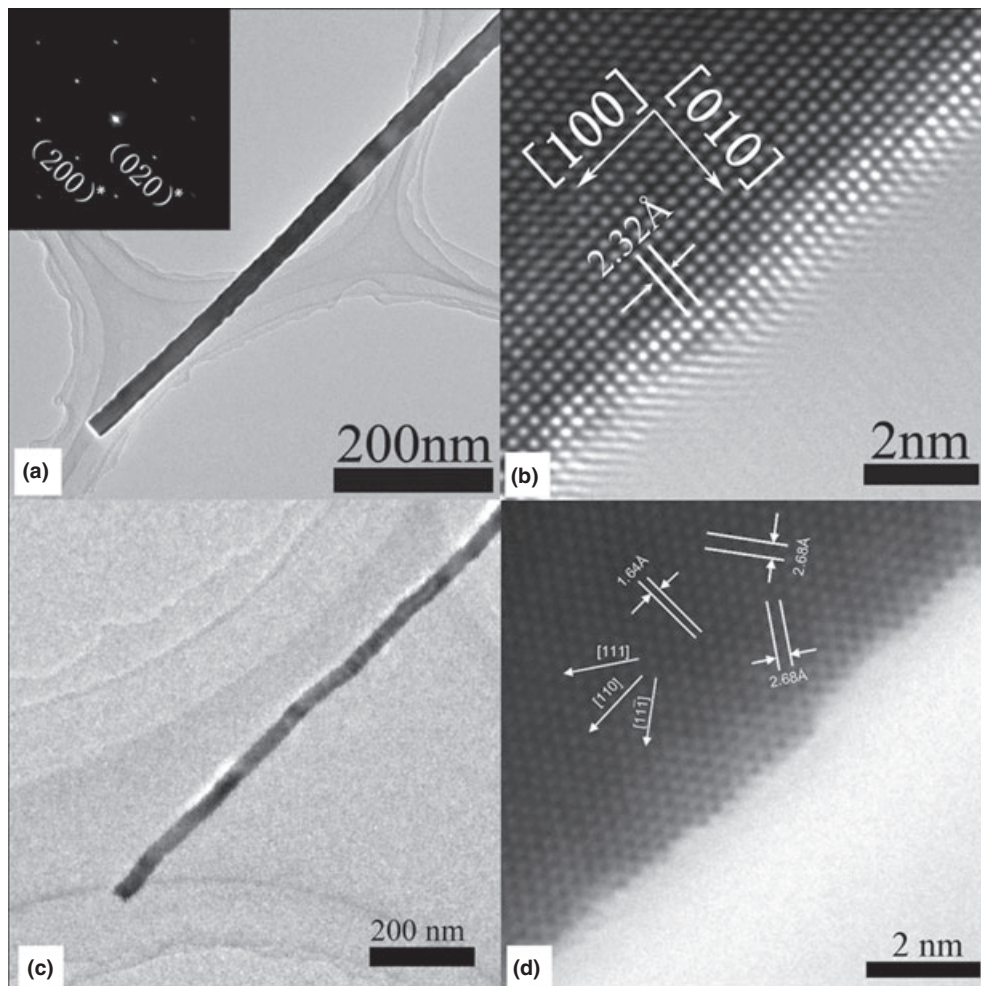


Fig. 3. (a) Low-magnification TEM image of a typical HfC nanowire. Inset is an SAED pattern taken from the nanowire. (b) HRTEM image of the nanowire showing clean surface. (c) Low-magnification TEM image of an HfC nanowire grown in [110] direction. (d) HRTEM image of the nanowire shown in (c).

with such a characteristic tip. This is possibly because of the process of Ostwald ripening occurred during the nanowire growth—the catalyst diffused from the tip of the nanowire onto the side surfaces. As a result, only a few of the nanowires can be observed with a catalyst at their tip. However, in this case, the nanowires should taper or have an enlargement in diameter at the tip.²² In our samples, nearly all of the nanowires have tips with a uniform diameter. So, here we conclude that it was not the Ostwald ripening that led to the disappearance of the catalyst, but the HCl generated in our system. As shown in reaction (1), the etchant HCl gas was generated during the synthesis and can remove the catalyst easily at high temperature. After the catalyst disappeared, the growth rate would become very slow so that the growth seemed to have stopped even before we turned off heating and cut off the reactant gas supply. To identify the role of Ni as catalyst, we conducted the experiment for a shorter reacting time to terminate the reactions before the catalyst was etched away. For this experiment, most of the nanowires obtained had a catalyst particle on the tip as shown in Fig. 4(a). From Figs. 4(b) and (c), which are the EDS data collected from the tip and body of a single nanowire, respectively, we can observe that the tip contained additional nickel (Ni) and oxygen (O) compared with the body of nanowire, which only contained Hf and C. The O may come from leaks of air during the second process of synthesis. This observation led to the conclusion that the HfC nanowire growth followed the VLS mechanism and Ni nanoparticles acted indeed as catalyst.

(3) Growth Process

The whole growth process of the HfC nanowires is suggested as follows: At the beginning, HfCl₄ whose melting point is only 432°C evaporated quickly and the vapors were carried over by H₂ to the substrate and mixed with CH₄. In the high-temperature zone, the mixed gases reacted through a reductive recombination process, which is similar to the reactions between ZrCl₄ and CH₄ proposed by Nartaowski *et al.*,²³ given in the partial reactions (2) and (3) below:



and



These two partial reactions lead to the total reaction given as reaction (1).

The intermediate product Hf and Ni formed alloys with a eutectic temperature lower than 1280°C according to their binary phase diagram.²⁴ It is also possible that the catalyst droplet is an alloy of Hf–Ni–C. Then the droplet appeared on the substrate to afford a preferential site for precipitation of HfC produced in the atmosphere. When the droplet became supersaturated, HfC nanowire began to grow layer by layer. The diameter of the nanowire is governed by the size of the droplet. During the growth of the HfC nanowire, the catalyst droplet was not stable all the time and the state

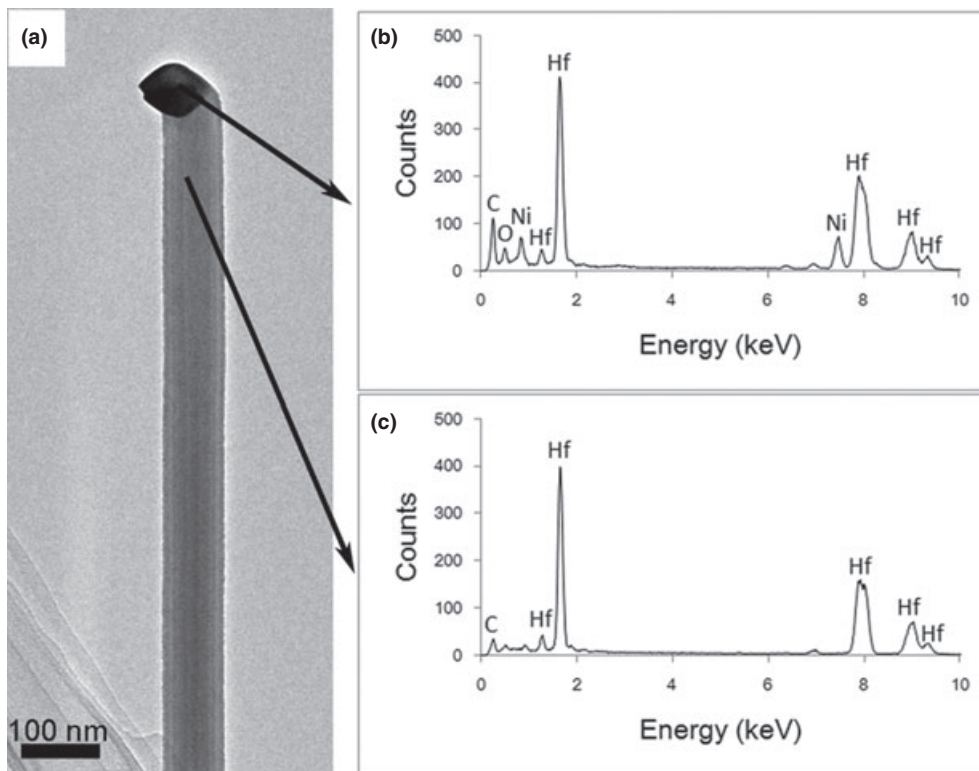


Fig. 4. (a) TEM image of a nanowire with Ni catalyst particle on the tip. (b) EDS analysis of the particle on the tip showing Ni and O as additional elements to the HfC nanowire. (c) EDS analysis of the nanowire body showing presence of only Hf and C.

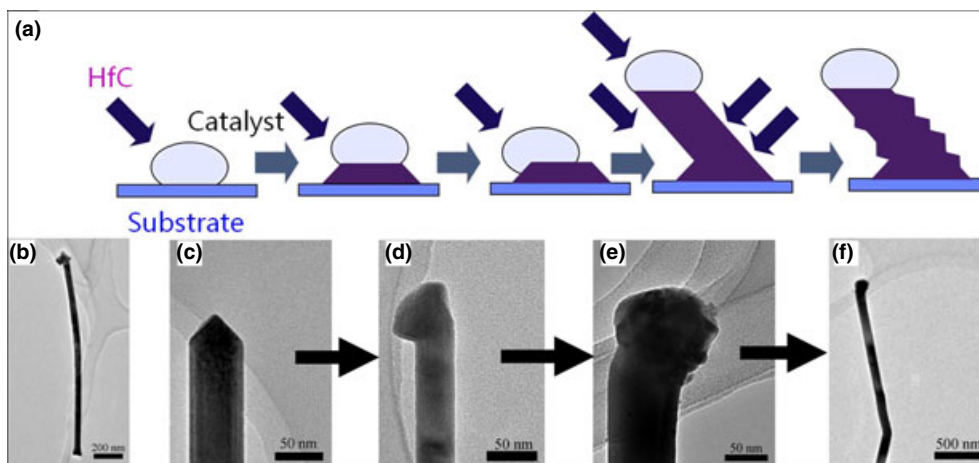


Fig. 5. (a) Schematic to describe the effect that changes of the catalyst on the morphology of nanowire. (b) A short nanowire with a ladder-shaped bottom. (c–f) Process for the formation of a kink. (c) The catalyst droplet stayed on its original direction. (d) The droplet moved aside. (e) The nanowire began to grow in a new direction. (f) A nanowire already had a kink and was to produce another one near the top.

of the droplet determined the geometry of the nanowire as illustrated in Fig. 5(a), similar to the model developed for the droplet-nanowire system by Schmidt *et al.* for the growth of Si nanowires with gold as catalyst.²⁵ As suggested by Schmidt *et al.*, before the contact point of the nanowire body, the catalyst droplet and the gaseous phases around it should have reached a balance and the growth process consists of several equilibrium states. In these states, the forces reached a static balance among the surface tension of the liquid droplet, the surface tension of the solid nanowire, and the interface tension between them. As a result, the area of the interface shrinks continuously with the changes as described by Schmidt *et al.*²⁵ and a ladder-shaped structure would form at the bottom of the nanowire, which was also observed on our nanowires as shown in Fig. 5(b). Moreover, if the growth process was disturbed by some factors difficult to control such as the turbulence in the reaction zone, the

composition of the catalyst droplet might change and interrupt the balance to cause changes in the droplet. The new wetting condition would in turn change the horizontal interfacial tension to a vertical force. The HfC accumulated on the new interface for growth and therefore kinks appeared on the nanowire. On the other hand, if the nanowire stopped growing axially, epitaxial growth resulted by residual product gases could occur and result in some zigzag structure on the side surface. In Figs. 5(c)–(f), nanowires at different growth stages when the reactions were terminated are shown to present a continuous process producing a kink. Figure 5(c) shows a straight nanowire without kink. In Fig. 5(d), the catalyst particle turned to one side to have a new wetting condition for equilibrium. Figure 5(e) shows that the nanowire began to grow in a new direction and it finished eventually as a kinked nanowire as shown in Fig. 5(f).

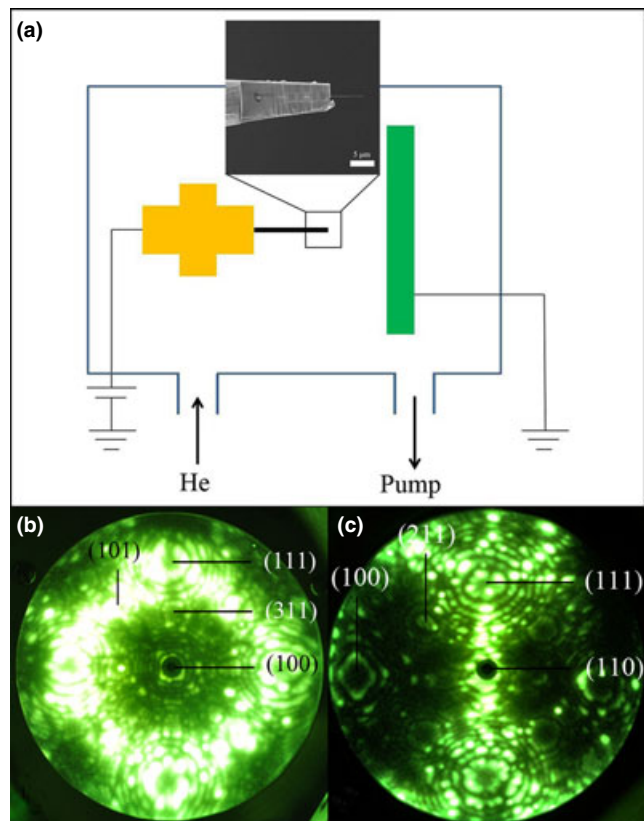


Fig. 6. (a) A simplified schematic of our field ion microscopy system. The inset is an SEM image showing the structure of the HfC probe. The HfC nanowire is picked up by our home-built nanomanipulator²⁷ and then fixed by C pads on a tungsten (W) tip with a flat cut by FIB. (b) FIM image obtained from a nanowire grown in [100] direction. (c) FIM image obtained from a nanowire grown in [110] direction.

(4) Field Ion Microscopy of HfC Nanowires

Field ion microscopy (FIM) is a powerful technique for surface characterization at atomic resolution and it is usually used to reveal the surface structure of the probe material. As illustrated schematically in Fig. 6(a), a positive high voltage is applied to the tip and a very strong electric field is produced at the vicinity of the tip where helium (He) atoms of the imaging gas are polarized in the electric field and are attracted to the tip. These polarized He atoms will eventually be ionized after colliding with the probe tip and then travel toward the phosphorous screen (or CCD detector) to form an FIM image. If the electric field is high enough, the surface atoms at the probe tip can also be ionized and subsequently be field-evaporated. Apparently, the contaminants and adsorbates will be evaporated first because of their weak bonding to the probe surface.²⁶ After field evaporation, clear and stable FIM images are usually obtained from clean surfaces as shown in Figs. 6(b) and (c). The circular rings indicate different facets produced in field evaporation. For a $\langle 100 \rangle$ -oriented HfC nanowire, the central facet is the {100} plane and the corners are {111} planes. Higher indexed planes are also resolved including the {311} and {101} planes. For a nanowire grown in the $\langle 110 \rangle$ direction, the central part is the {110} plane and the {111}, {100} and {211} planes are also observed in the FIM image as given in Fig. 6(c). In both FIM images, the {111} facets have the largest area, which means that the {111} planes have the highest atomic density.

IV. Conclusions

In conclusion, we have successfully synthesized single crystalline HfC nanowires with thickness of several tens of nanome-

ters and length of several tens of microns using a CVD method. Most of the nanowires are grown in the $\langle 100 \rangle$ direction and having clean as-grown surfaces. The growth process followed the VLS mechanism and the change of the catalyst caused the formation of kinks. The nanowires have also been made into FIM probes for characterization of surface structure and their growth directions.

Acknowledgments

This work was partially supported by the Development of System and Technology for Advanced Measurement and Analysis, Japan Science and Technology Corporation (JST) and the Nanotechnology Network Project of the Ministry of Education, Culture, Sports, Science, and Technology (MEXT), Japan.

References

- L. E. Toth, *Transition Metal Carbides and Nitrides*. Academic Press, New York, 1971, pp. 4–11.
- E. K. Storms, *The Refractory Carbide*. Academic Press, New York, 1964, pp. 35–46.
- K. J. Kagaric, G. G. Magera, S. D. Pollard, and W. A. Mackie, “Cold Field Emission from HfC (310),” *J. Vac. Technol. B*, **26** [2] 868–71 (2008).
- R. E. Krebs, *The History and Use of Our Earth's Chemical Elements: A Reference Guide*. Greenwood Press, Westport, 2006, pp. 147–50.
- M. J. L. Turner, *Rocket and Spacecraft Propulsion: Principles, Practice and New Development*. Springer-Praxis, Chichester, 2005, pp. 235–7.
- S. Motojima and Y. Kawashima, “Chemical Vapor Growth of HfC Whiskers and Their Morphology,” *J. Mater. Sci.*, **31**[14], 3697 (1996).
- X. Li, A. Westwood, A. Brown, R. Brydson, and B. Rand, “A Convenient, General Synthesis of Carbide Nanofibres Via Template Reactions on Carbon Nanotubes in Molten Salt Media,” *Carbon*, **47**[1], 201–8 (2009).
- H. Adachi, “Approach to a Stable Field Emission Electron Source,” *Scan. Electron. Microsc.*, **2**, 473–86 (1985).
- W. A. Mackie, J. L. Morrissey, C. H. Hinrichs, and P. R. Davis, “Field Emission from Hafnium Carbide,” *J. Vac. Sci. Technol. A*, **10** [4] 2852–6 (1992).
- W. A. Mackie, R. L. Hartman, and P. R. Davis, “High Current Density Field Emission from Transition Metal Carbides,” *Appl. Surf. Sci.*, **67** [1] 29–35 (1993).
- M. Yu, B. W. Hussey, E. Kratschmer, T. H. P. Chang, and W. A. Mackie, “Improved Emission Stability of Carburized HfC $\langle 100 \rangle$ and Ultrasharp Tungsten Field Emitters,” *J. Vac. Sci. Technol. B*, **13** [6] 2436–40 (1995).
- W. A. Mackie, T. Xie, J. E. Blackwood, S. C. Williams, and P. R. Davis, “Hafnium Carbide Thin Films and Film-Coated Field Emission Cathodes,” *J. Vac. Sci. Technol. B*, **16** [3] 1215–8 (1998).
- W. A. Mackie, L. A. Southall, T. Xie, G. L. Cabe, F. M. Charbonnier, and P. H. McClelland, “Emission Fluctuation and Slope-Intercept Plot Characterization of Pt and Transition Metal Carbide Field-Emission Cathodes in Limited Current Regimes,” *J. Vac. Sci. Technol. B*, **21** [4] 1574–80 (2003).
- V. N. T. Kuchibhatla, A. S. Karakoti, D. Bera, and S. Seal, “One Dimensional Nanostructured Materials,” *Prog. Mater. Sci.*, **52** [5] 699–913 (2007).
- S. R. Qi, X. T. Huang, Z. W. Gan, X. X. Ding, and Y. Cheng, “Synthesis of Titanium Carbide Nanowires,” *J. Cryst. Growth*, **219** [4] 485–8 (2000).
- C. H. Liang, G. W. Meng, W. Chen, Y. W. Wang, and L. D. Zhang, “Growth and Characterization of TiC Nanorods Activated by Nickel Nanoparticles,” *J. Cryst. Growth*, **220** [3] 296–300 (2000).
- T. Taguchi, H. Yamamoto, and S. Shamoto, “Synthesis and Characterization of Single-Phase TiC Nanotubes, TiC Nanowires, and Carbon Nanotubes Equipped with TiC Nanoparticles,” *J. Phys. Chem. C*, **111** [51] 18888–91 (2007).
- H. Zhang, Q. Zhang, J. Tang, and L.-C. Qin, “Single-Crystalline LaB₆ Nanowires,” *J. Am. Chem. Soc.*, **127** [9] 2862–3 (2005).
- H. Zhang, Q. Zhang, J. Tang, and L.-C. Qin, “Single-Crystalline CeB₆ Nanowires,” *J. Am. Chem. Soc.*, **127** [22] 8002–3 (2005).
- H. Zhang, Q. Zhang, G. Zhao, J. Tang, O. Zhou, and L.-C. Qin, “Single-Crystalline GdB₆ Nanowire Field Emitters,” *J. Am. Chem. Soc.*, **127** [38] 13120–1 (2005).
- R. S. Wanger, “VLS Mechanism of Crystal Growth”; pp. 47–119 in *Whisker Technology*, Edited by A. P. Levitt. Wiley, New York, 1970.
- F. M. Ross, “Controlling Nanowire Structures Through Real Time Growth Studies,” *Rep. Prog. Phys.*, **73** [11] 114501–21 (2010).
- A. M. Nartowski, I. P. Parkin, M. MacKenzie, A. J. Craven, and I. Macleod, “Solid State Metathesis Routes to Transition Metal Carbides,” *J. Mater. Chem.*, **9** [6] 1275–81 (1999).
- H. Okamoto, “HF-Ni (Hafnium-Nickel),” *J. Phase Equilibria.*, **14** [6] 769 (1993).
- V. Schmidt, J. V. Wittermann, and U. Gösele, “Growth, Thermodynamics, and Electrical Properties of Silicon Nanowires,” *Chem. Rev.*, **110**[1], 361–88 (2010).
- E. W. Müller, “Field Ion Microscopy,” *Science*, **149** [3684] 591–601 (1965).
- H. Zhang, J. Tang, J. Yuan, J. Ma, N. Shinya, K. Nakajima, H. Murakami, T. Ohkubo, and L.-C. Qin, “Nanostructured LaB₆ Field Emitter with Lowest Apical Work Function,” *Nano Lett.*, **10** [9] 3539–44 (2010). □